



Laser light scattering study of intrachain and interchain associations of poly(vinyl alcohol) in aqueous solution

Mingzhu Liu^{a,*}, Rongshi Cheng^b, Chi Wu^{c,d}

^aDepartment of Chemistry, Lanzhou University, Lanzhou 730000, People's Republic of China

^bDepartment of Chemistry, South China University of Technology, Guangzhou 510641, People's Republic of China

^cDepartment of Chemistry, The Chinese University of Hong Kong, Shatin, N.T., Hong Kong

^dThe Open Laboratory of Bond-selective Chemistry, Department of Chemical Physics, University of Science and Technology of China, Hefei 230000, People's Republic of China

Received 10 June 1997; accepted 8 October 1998

Abstract

Laser light scattering (LLS) was used to investigate the concentration dependence of intrachain and interchain associations of poly(vinyl alcohol) (PVA) in aqueous solution after different freezing-and-thawing cycles. Our results showed that if the PVA concentration (C) was much lower than its gelation concentration (C_{gel}), the average hydrodynamic size of the PVA chains became smaller after a cryogenic treatment, which was attributed to the change of the chain conformation from an extended coil to a compact globule because the static LLS results indicated that there was no change in the weight average molecular weight (M_w). This rules out a previously speculated degradation or scission of the PVA chains. When C was higher than C_{gel} , the apparent hydrodynamic size of the PVA chains was much larger and the scattering intensity became much stronger after the same cryogenic treatment, indicating the interchain association. © 1999 Elsevier Science Ltd. All rights reserved.

1. Introduction

Poly(vinyl alcohol) (PVA) in solution can form a gel under proper conditions. The PVA gel is so useful that its preparation and properties have been extensively studied in the past [1–9]. Shibatani [10] suggested that the crosslinking points in the PVA gel were syndiotactic sequences of six to eight monomer units on the basis of the macroscopic gel rigidity. Ogasawara [11] examined the syndiotacticity effects and found that the syndiotactic-rich PVA gel had a higher melting temperature and a higher elastic modulus than the atactic PVA gel. Komatsu et al. [5] investigated the relationship between the gelation and phase separation of PVA in water, concluding that the spinodal decompo-

sition had a significant effect on the gelation, but is not a necessary condition. Cha et al. [12] prepared a strong and transparent PVA gel with a high content of water and found that (1) the gelation was faster at lower temperatures; and (2) an increase of the PVA solution viscosity led to a weak PVA gel. Ohkura et al. [13] found a decrease of the gelation time at lower quenching temperatures and suggested that the crosslinking points in the PVA gel were made of the PVA crystallites after the study of the sol–gel transition of atactic PVA in a dimethyl sulphoxide and water mixture.

On the other hand, the intrachain crosslinking of PVA was studied first by Kuhn et al. [14] and then by Braun [15], Arbogast [16] and Gebben [17]. They found that the intrinsic viscosity decreases as the crosslinking density increases. A few years ago, Takigawa et al. [18, 19] examined the critical viscosity behavior of

* Corresponding author. Fax: +86-0931-8912582.

PVA in a dimethyl sulfoxide and water mixture near the gelation point and found that the shrinking of the PVA chains in dilute solutions is due to the formation of intrachain hydrogen bonding. In a previous paper [20], we reported two characteristic PVA concentrations, C_{gel} ($\sim 5 \times 10^{-5}$ g/ml) and C_{gel}^+ ($\sim 6 \times 10^{-2}$ g/ml); namely, when C approaches C_{gel} , the association of the PVA chains results in the formation of microscopic gels (clusters) which are not visible by eyes; and when C is higher than C_{gel}^+ , the polymer solution changes to a macroscopic gel if the solution temperature is low enough. In this study, using laser light scattering, we like to reveal the microscopic picture of the interchain and intrachain interactions of the PVA chains in aqueous solution. The details are as follows.

2. Experimental

2.1. Solution preparation

The poly(vinyl alcohol) (PVA) sample employed in this work was a commercial product. The nominal degree of polymerization and saponification of the poly(vinyl alcohol) (PVA) used was ~ 2450 and ~ 98 mol%, respectively. The intrinsic viscosity $[\eta]$ was 97 ml/g. The overlap concentration C^+ estimated from the reciprocal of $[\eta]$ was 1.03×10^{-3} g/ml. The weight average molecular weight (M_w) of the sample, determined by static laser light scattering was 1.14×10^5 g/mol. The PVA stock solution (5×10^{-3} g/ml) was prepared by the dissolution of a proper amount of PVA in deionized water under reflux for 2 h. The stock solution was further diluted into a desired concentration in the range 1×10^{-6} – 5×10^{-3} g/ml.

2.2. Freezing-and-thawing treatment

The freezing process varied depending on the freezing temperature. The PVA solution in a 10-ml flask was placed in a freezer at -23°C for 15 h, or immersed into liquid nitrogen for 5 min. The thawing was always done at 20°C for 9 h.

2.3. Laser light scattering (LLS)

A commercial LLS spectrometer (ALV/SP-150 equipped with an ALV-5000 multi- τ digit correlator) was used with solid-state laser (ADLAS DPY425 II, output power ≈ 400 mW at $\lambda = 532$ nm) as the light source. All the LLS experiments were done at $25 \pm 0.1^\circ\text{C}$. In static LLS, the angular dependence of the excess absolute time-averaged scattered intensity, known as the excess Rayleigh ratio [$R_{\text{vv}}(\theta)$], was measured. The measurement of a set of dilute solutions at different scattering angles can lead to the weight

average particle molecular weight M_w , the second-order virial coefficient A_2 ; and the root-mean-square z -average radius R_g [21]. Five PVA solutions in the concentration range 1×10^{-4} – 5×10^{-3} g/ml were used for static LLS. The intensities of the light scattered from the PVA solutions at different scattering angles (6 – 20°) were measured. The specific refractive index increment dn/dC for PVA in water at 25°C and $\lambda = 532$ nm is 0.159 ml/g.

In dynamic LLS, the PVA solutions ($C = 1 \times 10^{-6}$, 1×10^{-4} and 5×10^{-3} g/ml) before and after the freezing-and-thawing cycles were measured. The Laplace inversion of the intensity–intensity time correlation function $G^{(2)}(t, \theta)$ can lead to a line-width distribution function $G(\Gamma)$ [22, 23]. For a pure diffusional relaxation, Γ is proportional to the translational diffusion coefficient D which is further reciprocally proportional to the hydrodynamic radius R_h , or in other words, a smaller R_h results in a larger Γ . All the PVA solutions were filtered by a $0.5 \mu\text{m}$ Millipore filter in order to remove dust, and were measured at 25°C .

3. Results and discussion

Fig. 1 shows the line-width distributions $G(\Gamma)$ of the PVA solution ($C = 1 \times 10^{-6}$ g/ml). $G(\Gamma)$ shifted to the high Γ direction after different freezing-and-thawing cycles. The corresponding average hydrodynamic radii (R_h) were 15.0, 13.3 and 9.5 nm before and after the freezing-and-thawing cycles, respectively. It should be stated that there was no change in the scattering intensity (i.e. no change in the chain molar mass) after the freezing-and-thawing cycles, indicating that the change involves only individual PVA chains, i.e. the chain changes from an extended coil to a shrunken confor-

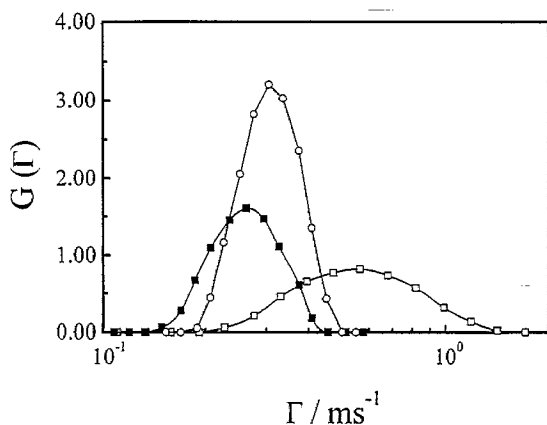


Fig. 1. Line-width distribution $G(\Gamma)$ of the PVA solution, where $C = 1 \times 10^{-6}$ g/ml. (■) Before freezing; (○) frozen once to -23°C and (□) frozen once in liquid nitrogen.

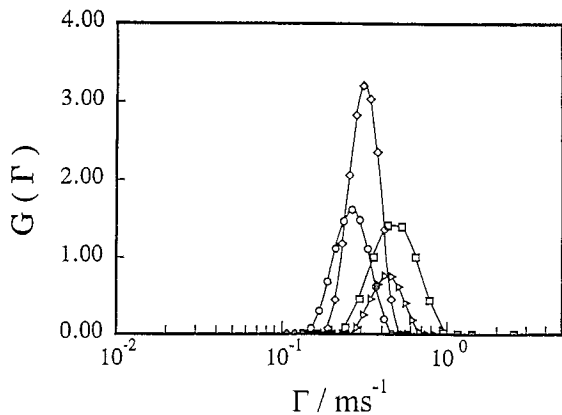


Fig. 2. Line-width distribution of the PVA solution, where $C = 1 \times 10^{-6}$ g/ml. \circ , \diamond , \triangle and \square denote before freezing and after freezing 1, 3 and 5 times to -23°C , respectively.

mation. This is why R_h decreases as the freezing temperature.

Further, Fig. 2 shows that the longer the freezing time, the more $G(\Gamma)$ shifted toward the high Γ direction. The corresponding values of R_h were 15.0, 13.3, 10.5 and 8.7 nm, respectively. Fig. 3 shows that when the PVA concentration was 1×10^{-4} g/ml, $G(\Gamma)$ became a bimodal distribution after the freezing-and-thawing cycles. The second peak with a lower Γ , i.e. a slower diffusion, indicates the formation of larger interchain aggregates, which were also evidenced by an increase in the scattering intensity.

Fig. 4 shows that $G(\Gamma)$ shifted slightly toward the higher Γ direction after 1 h freezing. As the freezing time increased, $G(\Gamma)$ became a bimodal distribution. As discussed before, the peak with a lower Γ indicates the formation of large intrachain aggregates. Fig. 4

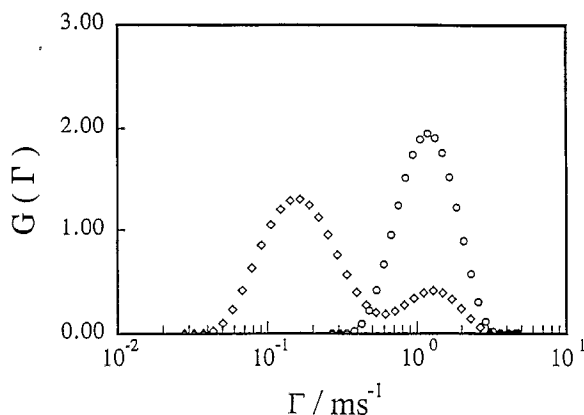


Fig. 3. Line-width distribution of the PVA solution, where $C = 1 \times 10^{-4}$ g/ml. \circ before freezing; and \diamond frozen three times to -23°C .

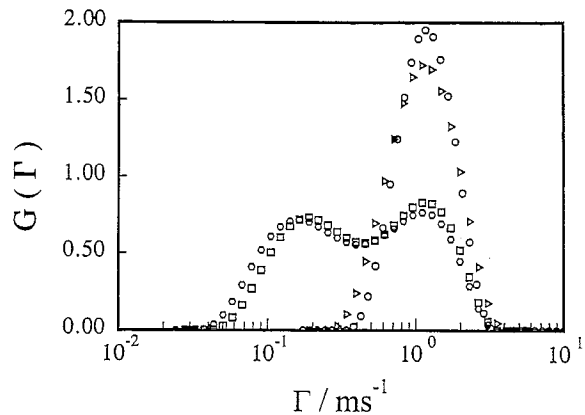


Fig. 4. Line-width distribution of the PVA solution, where $C = 1 \times 10^{-4}$ g/ml. \circ , \diamond , \triangle and \square denote before freezing and after freezing for 1, 3 and 15 h at -23°C , respectively.

also shows that there is basically no difference between 3 h and 15 h freezing. This is understandable because each PVA chain could only collapse to a finite size. Moreover, in the process of the experiment, we found that the gelation time decreased with the freezing temperature, similar to the results reported by Ohkura et al. [13].

Fig. 5 shows that, after heating to 80°C for 2 h, $G(\Gamma)$ returned to a unimodal distribution, indicating that the interchain aggregates (related to the second peak) formed after the freezing-and-thawing cycles could be destroyed at 80°C . Further, Fig. 6 shows that the second peak in $G(\Gamma)$ formed after the freezing-and-thawing cycles can be removed by a $0.02 \mu\text{m}$ Millipore filter, indicating that the peak with a low Γ value was related to large interchain aggregates. It should be stated that both the interchain aggregates and the collapsed intrachain globules were very stable at room

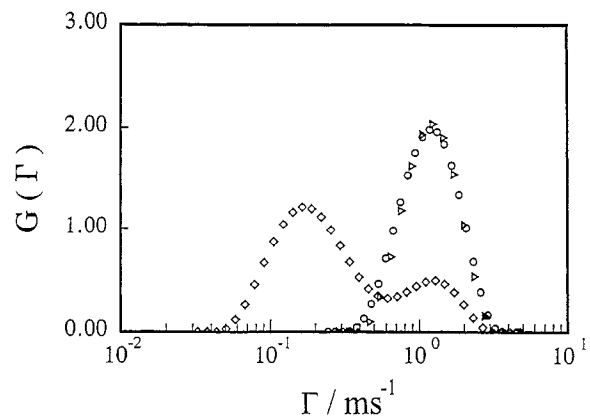


Fig. 5. Line-width distribution of the PVA solution, where $C = 1 \times 10^{-4}$ g/ml. \circ before freezing; \diamond after freezing five times in liquid nitrogen; \triangle heated to 80°C for 2 h after freezing the PVA solution in liquid nitrogen five times.

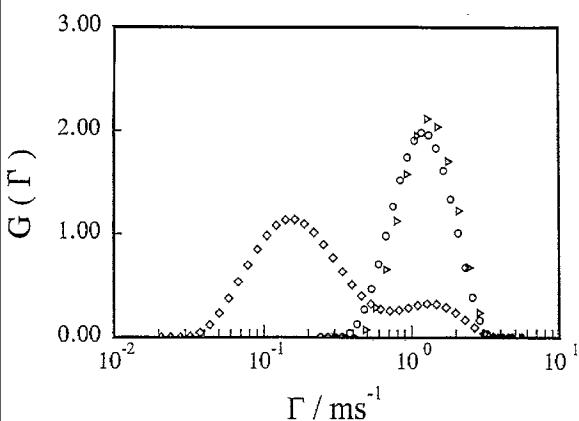


Fig. 6. Line-width distribution of the PVA solution, where $C = 1 \times 10^{-4}$ g/ml. (○) before freezing; (◇) after freezing three times to -23°C ; and (△) filtered by a $0.02 \mu\text{m}$ filter after freezing the PVA solution three times to -23°C .

temperature because there was no change in $G(\Gamma)$ even a few days after the freezing-and-thawing cycles.

In summary, the intrachain interaction is dominated in the freezing-and-thawing cycles if the PVA solution is very dilute, i.e. the PVA concentration (C) is much lower than the gelation concentration (C_{gel}). The intrachain interaction is presumably through the hydrogen bonding between the pendent hydroxyl groups on the PVA chain backbone. The intrachain interaction actually leads to the coil-to-globule transition of individual PVA chains. When C is higher than C_{gel} , the interchain aggregation becomes dominate. Our results showed that both lowering the freezing temperature and repeating the freezing-and-thawing cycle can increase the intrachain contraction and interchain aggregation. Our results have ruled out the previously suggested degradation or scission of the PVA chains in the freezing-and-thawing cycles. The interchain aggregates and the collapsed interchain globules formed in the cryogenic process are stable at ambient temperatures.

Acknowledgements

The Chinese National Basic Research Project "Macromolecular Condensed State" is gratefully acknowledged. Wu likes to acknowledge the National

Distinguished Young Investigated Fund (1996, 29625410). The authors thank Ms S. F. Peng for drawing the figures and typing the revised manuscript.

References

- [1] Peppas NA, Merrill EW. *J. Polym. Sci., Polym. Chem. Edn* 1976;14:441.
- [2] Matsuzawa S, Yamaura K, Kobayashi H. *Colloid Polym. Sci.* 1981;25:1147.
- [3] Watase M, Nishinari K. *Makromol. Chem.* 1985;186:1081.
- [4] Watase M., Nishinari K. *J. Polym. Sci., Polym. Phys. Edn* 1985;23:1083.
- [5] Komatsu M., Inoue T., Miyasaka K. *J. Polym. Sci., Polym. Phys. Edn* 1986;24:303.
- [6] Lozinsky VI, Vainerman ES, Domotenko LV, et al. *Colloid Polym. Sci.* 1986;264:19.
- [7] Yamaura K, Katou H, Tanigami T, et al. *J. Appl. Polym. Sci.* 1987;34:2347.
- [8] Domszy RC, Alamo R, Edwards CO, et al. *Macromolecules* 1986;19:310.
- [9] Toshihiro H, Hidetoshi M, Takashi S, Sadao H. *J. Appl. Polym. Sci.* 1992;45:1849.
- [10] Shibatani K. *Polym J* 1970;1:348.
- [11] Ogasawara A, Nakajima T, Yamaura K. *Colloid Polym. Sci.* 1975;57:145.
- [12] Cha WI, Hyon SH, Ikada Y. *Makromol. Chem.* 1992;193:1913.
- [13] Ohkura M, Kanaya T, Kaji K. *Polymer* 1992;33:3686.
- [14] Kuhn W, Balmer G. *J. Polym. Sci.* 1962;57:311.
- [15] Braun D. *Angew. Chemie* 1976;15(8):451.
- [16] Arbogast W, Hortath A, Vollmert B. *Makromol. Chem.* 1980;181:1513.
- [17] Gebben B, Van den Berg Hans WA, Bargeman D, Smolders CA. *Polymer* 1985;26:1737.
- [18] Takigawa T, Urayama K, Masuda T. *Chem. Phys. Lett.* 1990;174(3–4):259.
- [19] Takigawa T, Urayama K, Masuda T. *J. Chem. Phys.* 1990;93(10):7310.
- [20] Mingzhu Liu, Rongshi Cheng, Renyuan Qian. *J. Polym. Sci. Part B: Polym. Phys.* 1995;33:1731.
- [21] Zimm BH. *J. Chem. Phys.* 1948;16:1099.
- [22] Chu B. *Laser Light Scattering*. New York: Academic Press, 1974.
- [23] Chu B, Pecora R. *Dynamic Light Scattering*. New York: Plenum Press, 1976.